Section A-Research paper

One pot Facile Fabrication and Characterization of Ag-Fe Nanocomposite- As photocatalytic removal of methyl red dye and pharmacological applications

Poongodi Vijayakumar and Swaminathan Senguttuvan*

PG & Research Department of Chemistry, Thiru.Vi.Ka.Government Arts College (*Affiliated to Bharathidasan University*),

Thiruvaru, India.

Corresponding Author: Senguttuvan Swaminathan & senguttuvanathan@gmail.com

Abstract

This article report is based on the novel synthesis of Ag Nps (TA), Fe Nps (TF) and Ag-Fe Nps (TAF) nanocomposites, using ethanolic extract of *Clitoria ternatea* as a bio-reductant and characterized by various spectral techniques such as UV-visible spectrophotometry (UV), Fourier transform infrared spectrometry (FT-IR), Scanning electron microscopy (SEM) and Energy dispersive micro analysis (EDAX). The synthesized bimetallic nanocomposite TAF was investigated for its pharmacological efficacy. The synthesized TAF bimetallic nanocomposite has been subjected to analyse its potential as photocatalyst in the removal of methyl red dye.

Keywords: *Clitoria ternatea*, anti-biofilm, anti-inflammatory, SEM, EDAX, photocatalytic degradation.

1. Introduction

Nanostructures are based on the influence of individual atoms or molecules to produce materials for functioning well below the nanometre 100 nm[1-5]. A new branch of scientific endeavour called green nanotechnology starts emerging and developing as one of the frontiers of science and engineering today [6-10]. Many innovative inventions are emerging every day in the field of nanoscience for the betterment of the society. The present report aims at green synthesis of bimetallic (Ag-Fe) nanoparticles and its characterisation. Here, the green synthesis refers to the usage of bio-reductant as capping reagents instead of environmentally hazardous chemicals. Many researches were carried out in synthesizing

various nanoparticles using varieties of plant extract as bio-reductant and stabilizing agent. Each nanoparticle has its very own potential and utilised in different fields of applications. Now, one such new trends is the fabrication of bimetallic nanoparticles over monometallic nanoparticles using bio-reductant due to their superior optical properties and catalytic activities. Bimetallic nanoparticles are the combination of two different metals have drawn a greater attention among the young researchers than the monometallic nanoparticles based on both the scientific as well as technological point of view [11-15]. Generally, bimetallic nanoparticles are prepared by simultaneous reduction of two metal ions in the presence of appropriate stabilization techniques such as static-electronic repulsive force and steric hindrance [16-20]. By governing the size, shape and structure of the nanoparticles, we can control over the reduction rates of the two metal ions [21-25]. The bimetallic nanoparticles offers the tendency of optimization of the energy of plasmon absorption band of metallic mixture which serves as a multipurpose tool for biosensing. These properties may differ from those of pure elemental particles and include unique size dependent optical, electronic, thermal, and catalytic effects of the metal ions [25-31]. Because, bimetallic nanocomposites have greater surface area which increases their adsorption power and hence acts as efficient catalysts [32-36]. This makes them to play a key role in various fields.

2. Experimental Methods

2.1. Preliminary qualitative phytochemical investigation

The plant *Clitoria ternatea* was collected from *Pachaimalai* hills near Tiruchirappalli district located at 119^0 N, 78^0 210 E of Tiruchirappalli, Tamil Nadu, India. The leaves were washed thoroughly dried under shade. About 25 g of the powdered leaf was extracted in 250 mL of ethanol under soxhlet method. The extract was stored in an amper bottle and refrigerated. The extract is taken for phytochemical screening [37,38].

2.2. Bio-fabrication of Ag Nps, Fe Nps and Ag-Fe nano particles Using leaf extract as Bio-reductant

Five different concentrations of ethanolic leaf extract (20 to 60 µm) were prepared using double distilled water. Silver nitrate, ferric chloride solutions were taken along with each concentration of leaf extract solutions in different reaction bottles where the pH of the reaction mixture was altered by the addition of NaOH till it attains more than 12.5 to aid the formation of nanoparticles. The reaction mixtures were kept in the magnetic stirrer maintained at $70\ ^0$ C for 3 hours. The color change of the solution in the reaction mixture indicates the formation of nano particles were followed drying with muffle furnace at

temperature of 600 ^{0}C and then subjected to characterization [39, 40] and further investigated for industrial and pharmacological applications.

2.3. Bimetallic nanocomposite as a catalyst in the removal of Methyl Red Dye - Photocatalytic degradation

The photo-catalytic behaviour was evaluated by the elimination of Methyl red dyes (10 ml of aqueous solution of dyes dissolved 0.05g) under UV light or sunlight radiation. The light source used was a 150 W Xe (Xenon) lamp, and the distance between the UV source and the photo-reaction vessel was 10 cm. Prior to irradiation, the suspensions were magnetically stirred in the dark for 30 min. Then, the photoreaction vessel was exposed to UV irradiation. The selected dyes were used in conjunction with 50mg of catalyst sample in the photo-removal experiment. At regular time intervals, 3 ml of the suspension was taken for centrifugation to separate the photo catalyst and for further evaluation using a UV-Vis absorption spectrometer.

2.4. Potential of bimetallic nanocomposite in Pharmacological Applications

2.4.1. Anti-inflammatory

Denaturation of proteins is the reason of inflammation. Inhibition of protein denaturation was evaluated by adding 500 µL of 1% bovine serum albumin to bimetallic nanocomposites (500, 250, 100, 50 and 10 µg/mL). This mixture was kept at room temperature for 10 minutes, followed by heating at 51°C for 20 minutes. The resulting solution was cooled and then the absorbance was recorded at 660 nm. Acetyl salicylic acid was taken as a positive control[41-45].

2.4.2. Anti-diabetic

The α- amylase inhibitory activity was assessed by subjecting the analyte at various concentrations was remixed with 200 µl of α- amylase solution (1.0 U/ml in phosphate buffer pH 6.9), and incubated at 25^{o}C for 30 min. After pre-incubation, 400 µl of 0.25 % starch solution in the phosphate buffer (pH 6.9) was added to each analyte of various concentration to initiate the reaction[46-49]. The reaction was carried out at 37^{o}c for 5 min and terminated by the addition of 1.0 ml of the DNS reagent. The test tubes were then kept over a boiling water bath for 10 min and cooled to room temperature. The reaction mixture was then diluted and absorbent (A) was measured at 540 nm.

2.4.3. Anti-bacterial

The bacterial strains such as *Staphylococcus aureus*- 902, *Aeromonas hydrophila, Proteus vulgaris*- 426 and *Streptococcus pyogenes*- 1928 were used to investigate the anti-bacterial

ability of the synthesized bimetallic nanocomposite by well diffusion method. The plates were then incubated at 37°C for 24 hours. The antibacterial activity was assayed by measuring the diameter of the inhibition zone formed around the wells[50-52]. Gentamicin antibiotic was used as a positive control. The values were calculated using Graph Pad Prism 6.0 software (USA).

2.4.4. Antifungal

The fungal strains such as *Candida albicans, Aspergillus aculeatus, Cryptococcus neoformans and Aspergillus niger* were taken to check the anti-fungal efficacy of the fabricated bimetallic nanocoposites by well diffusion method. The plates were then incubated at 28°C for 72 hours. The anti-fungal activity was assayed by measuring the diameter of the inhibition zone formed around the wells. Amphotericin B was used as a positive control[53]. The values were calculated using Graph Pad Prism 6.0 software (USA).

2.4.5. Anti-Biofilm Assay

To evaluate the efficacy of the synthesized bimetallic nanocomposite in interrupting biofilm formation, MTP assay was carried out accordingly using 96 well-flat bottom polystyrene titre plates. Individual wells were filled with 180 µL BHI broth followed by inoculation with 10 µL of overnight pathogenic bacterial culture. To this 10 µL of TAF was added from the prepared stock solution of 500, 250, 125, 62.5 and 31.25 µg/mL respectively along with control and incubated at 37°C for 24 h. After incubation, the adherence of sessile bacteria was fixed. Excessive stain was removed by deionized water wash and kept for drying. Further, dried plates were washed with 95% ethanol and optical density was determined using a microtitre plate reader (Thermo) at 600 nm. The percentage of biofilm inhibition was calculated using the below formula [54- 56].

% Biofilm inhibition = [(Control OD- Test OD/ Control OD)] × 100

3. Results and Discussion

3.1. Preliminary qualitative phytochemical investigation

The results of the preliminary phytochemical screening of the ethanolic extract of the leaves of *Clitoria ternatea* are shown in Table-1. It illustrates that the active phyto compounds such as alkaloids, terpinoids, flavanoids, phenolic compounds, proteins etc. are present except Non-reducing sugar, tyrosine, steroids and cyanogenic glycosides. The

presence of these active compounds is responsible for the active potential of the plant extract in various fields of applications.

Phyto-constituents	Inferrence	Phyto-constituents	Inferrence
Carbohydrates	+	Anthraquinone Glycosides	+
Reducing Sugar	+	Saponin Glycosides	+
Hexose Sugar	+	Cyanogenic Glycosides	-
Non-Reducing Sugar (Starch)	-	Alkaloids	+
Proteins	+	Tannins	+
Amino Acids	+	Phenolic Compounds	+
Tyrosine	-	Flavonoids	+
Steroids	-	Terpenoids	+
Glycosides	+	Saponins	+

Table (1): Qualitative preliminary phytochemical screening of ethanolic extract of *Clitoria ternatea*

+ Present - Absent

3.2. Gas Chromatography- Mass Spectrum Study (GC-MS)

The GC-MS chromatogram of the *Clitoria ternatea* ethanolic leaves extract showed twenty peaks which indicates the presence of active phyto constituents (Fig.2). On comparison of the mass spectra of the constituents with the NIST and WILEY libraries the predominant constituents were characterized and identified. Among the twenty constituents the following compounds were found to be predominantly present such as Cyclohexanone (52.09 %), 1,2-Benzenedicarboxylic Acid (11.69 %), Pentadecane (7.4%), Octadecane (4.61%) and dl-c-Allylglycine (1.46%)

.

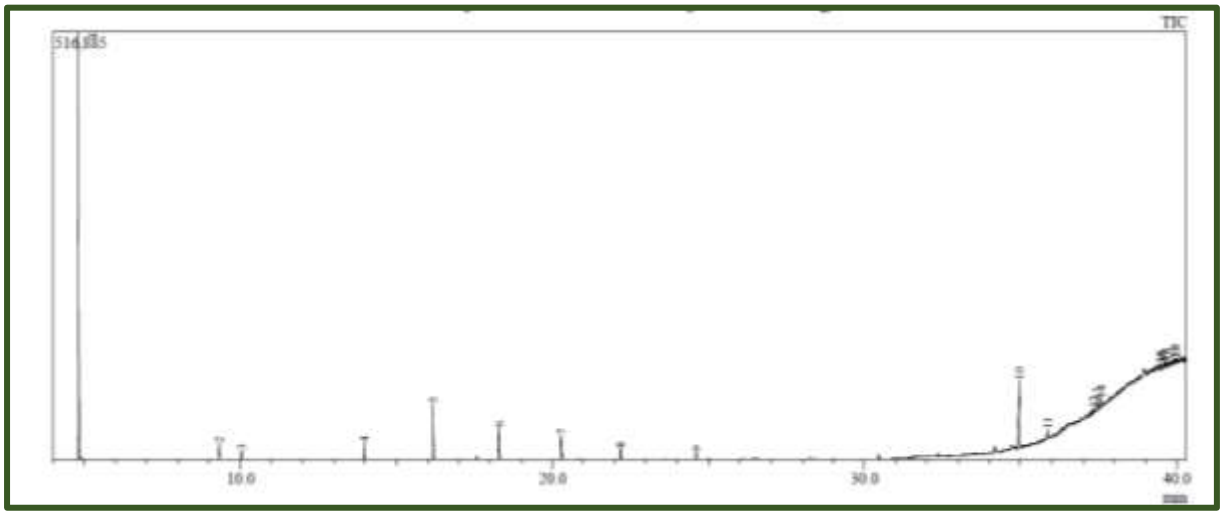

Figure-2: GC-MS Chromatogram of the ethanolic leaf extract of Clitoria ternatea

3.3. Fourier Transform Infra-Red Spectroscopy (FTIR)

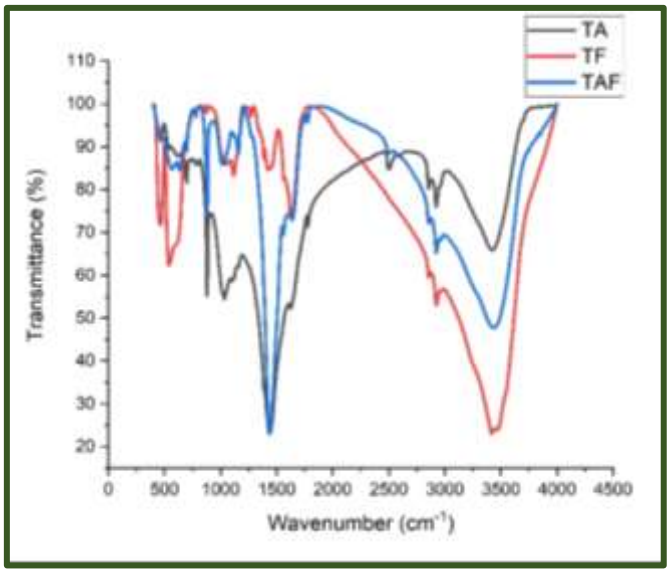

Figure-3: FT-IR Correlation Spectra of TP-plant extract, TP- Ag Nps, TP- Fe Nps and TAF-bimetallic nano-composite

The FT-IR was used to identify the functional groups which are responsible for capping and stabilization of the nanoparticle by the reduction of Ag^{+} higher oxidation state into Ag^{0} a lower oxidation state. In the present investigation, the FT-IR spectrum of TA nanoparticles (Ag Nps) showed various bands at 879.63 cm^{-1}, 1033.63 cm^{-1}, 1625.00 cm^{-1}, 2922.15 cm^{-1} and 3418.26 cm^{-1} (Fig.3) [57-58]. The band obtained at 879.63 cm^{-1} corresponds to C-C stretching vibration. The bands at 2922.15 cm^{-1} and 1033.63 cm^{-1} are may be due to C-H stretching and C-O stretching respectively [59].

FTIR spectrum was taken to pick out the potential functional groups responsible for the synthesis of TF NPs. The bands at 3414.23 cm^{-1} represent the characteristic band of OH stretching [60]. The bands at 1421.05 cm^{-1} and 1116.93 cm^{-1} were may be due to C–N stretching of amines and C–O stretcthing [60]. The peak at 2923.34 cm^{-1} showed the presence of C-H stretching [61]. The peak at 539.15 cm^{-1} and 465.10 cm^{-1} indicated the existence of Fe–O stretching in TFNPs [62, 63]. Based on these FTIR spectrum, the biomolecules consisting of functional groups such as –OH, C-H, C-O, C-N were responsible for the formation of TFNPs are confirmed.

The fabricated Ag, Fe, and Ag–Fe bimetallic nanoparticles with the extract, the FTIR spectra were correlated to identify the variation of the frequencies were band has observed. This spectral report consists of that the extract capped nanoparticles, the reduced state metal ions, and stabilized the monometallic as well as bimetallic nanoparticles during the synthesis with the enhanced efficacy. The TAF nanoparticles FT-IR spectrum depicts various bands at 880.31 cm^{-1}, 1776.09 cm^{-1} and 2923.28 cm^{-1}. The band at 880.31 cm^{-1} corresponds to C–C vibration. The band at 2923.28 cm^{-1} due to the C–H stretching. The bands at 3434.08 cm^{-1} represent the phenolic OH group. The bands at 1438.17 cm^{-1} and 1019.33 cm^{-1} peaks may be due to C–N stretching and C–O stretching respectively [61]. The peak at 563.80 cm^{-1} indicated the existence of Fe–O stretching in TAFNPs [62, 63].

3.4. UV-Visible

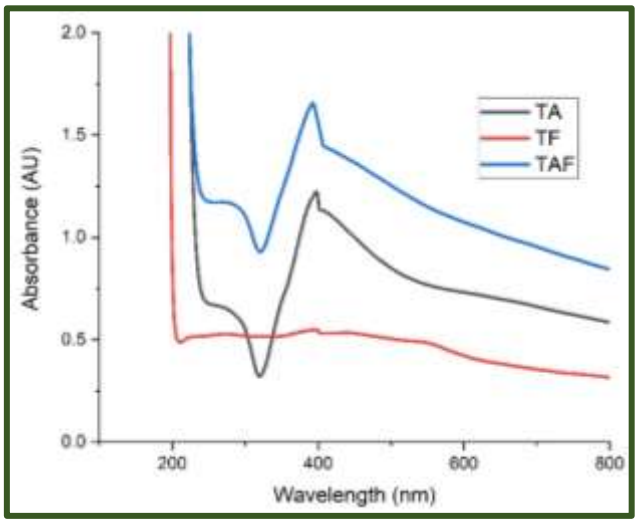

Figure-4: UV-Visible Correlation Spectra of TA- Ag Nps, TF- Fe Nps and TAF- bimetallic nano-composite

The leaves of *Clitoria ternatea* were used for the bio-reduction of $AgNO_3$ into the nanoscale level. TA NPs were confirmed by the absorbance measured in the UV–Visible spectrometry at 396.30 nm (Fig.4).

The UV−visible spectrum of the prepared TF NPs was recorded as a function of wavelength range from 400-800 nm (Fig. 4). The colour change indicated the formation of TF NPs during the synthesis and the absorbance recorded for TF NPs was 274.90 nm. Bimetallic nanoparticles has enhanced properties and applications due to the synergism aroused from the combination of two different metals. Many investigations has been carried out on monometallic nanoparticles but only fewer work has been established in bimetallic. In the case of the Ag-NPs, Fe-NPs and the synthesis of Ag–Fe bimetallic nanoparticles, all the three nanoparticles depicted the characteristic UV–Vis spectral peak, 392.55 nm (Fig. 4). Thus the correlation of UV–Vis absorption spectra for the silver, iron and bimetallic nanoparticles has depicted. However, for the bimetallic nanoparticles, an absorption spectrum suggested the formation of silver-iron core–shell bimetallic nanoparticles.

3.5. DLS Analysis

The report of the Dynamic Light Scattering (DLS) method determines the size, polydispersity index and diffusion constant for the bio-synthesized TA Nps, TF Nps and TAF Nps.

The DLS report of the synthesized individual monometallic and bimetallic nanocomposites were depicted in (Fig.5) which depicts the details such as size, polydispersity index and diffusion constant. The size of the capped TA NPs, TF NPs and TAF NPs were 66.1 nm, 100nm and 66.8 nm respectively. The polydispersity index recorded for the bio-reducted TA NPs, TF NPs and TAF NPs were 0.290, 0.296 and 0.345 respectively. Similarly, the diffusion constant measured for the synthesized individual monometallic and bimetallic nanoparticles were $7.447e^{-008}$ cm²/sec , $4.878e^{-008}$ cm²/sec and $7.359e^{-008}$ cm²/sec.

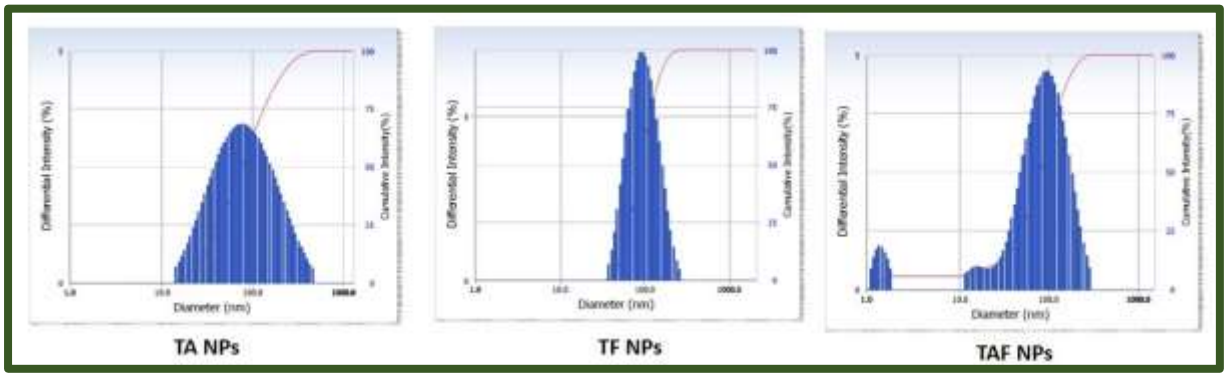

Figure-5: EDAX Spectra of a) TA- Ag Nps, b) TF- Fe Nps and c) TAF- bimetallic nano-composite

3.6. SEM Analysis

The SEM analysis report clearly posturize the spherical shape with the average size of 76nm in Fig.6 [a,b] indicates the fabrication of bio-reducted silver nanoparticles (TA Nps). Similarly, flakes like particles indicates the formation of capped iron nanoparticles (TF Nps) in Fig. 6 [c,d]. The clear depiction of mixture of cuboid and flakes confirms the formation of bimetallic nanocomposite TAF Nps in Fig.6[e,f].

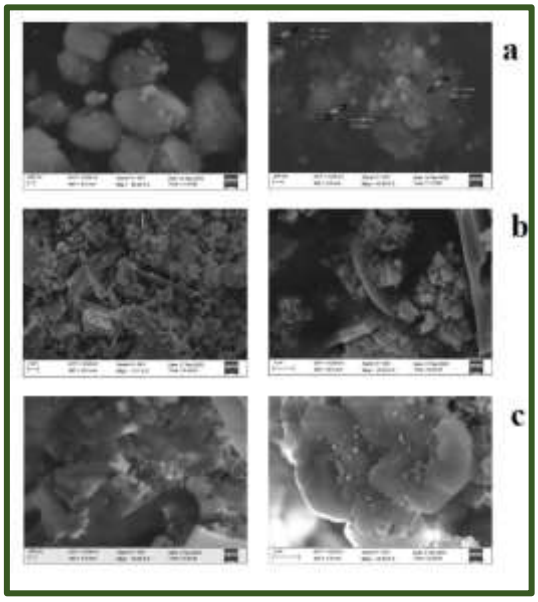

Figure-6: SEM images of [a] TA- Ag Nps, [b] TF- Fe Nps and [c] TAF- bimetallic nano-composite

3.7. Bimetallic nanocomposite as a catalyst in the removal of Methyl Red Dye -Photocatalytic degradation

Initially the methyl red dye did not undergo any degradation under UV-light radiation. In the similar experimental manner the removal efficacy of the synthesized TAF NPs (Ag-Fe NPs) on methyl red dye was tested. The colour of the dye solution faded on adding the

bimetallic nanoparticles. The photo-removal efficiency percentage was calculated for regular interval of time (1, 2, 3, 4 hrs). The photo-removal efficiency values are tabulated in Table-2. From the various concentration of the bimetallic nanoparticles (10, 50, 100, 250 and 500 µg/ml) at 500 µg/ml upto 4hrs the photo-removal efficiency percentage was found to be 30.612%. Thus TAF NPs is a concentration and time dependent photo-removal efficient. Since as the concentration and time increases the dye removal capability also increases.

Table-2: Photocatalytic Activity

S. No	% of different Time interval (hours)	% of Photo removal efficiency (µg/ml)				
		500 µg/ml	250 µg/ml	100 µg/ml	50 µg/ml	10 µg/ml
1.	Initial	25.510	20.918	18.367	15.306	8.163
2.	1 hrs	27.040	22.448	19.897	15.816	9.693
3.	2 hrs	27.551	23.469	20.408	17.346	15.306
4.	3 hrs	29.591	25	22.959	17.857	16.326
5.	4 hrs	30.612	28.061	25	22.959	16.836

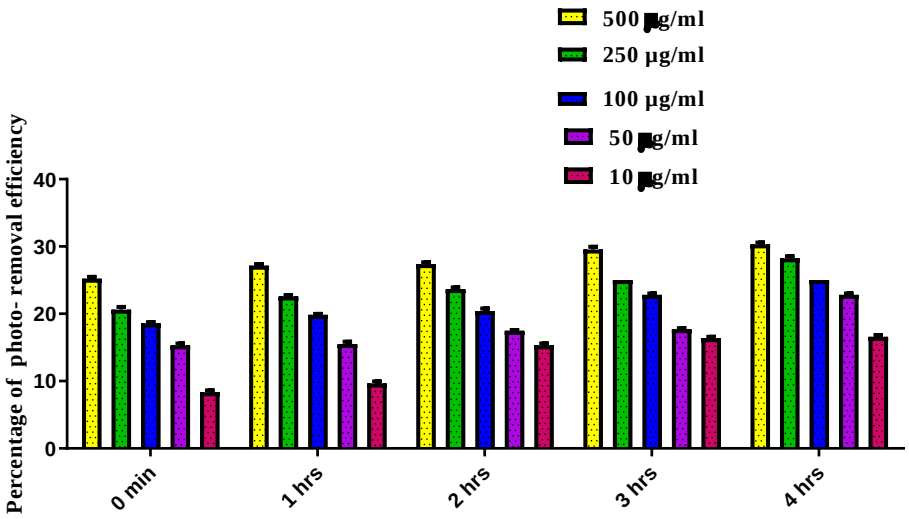

Figure-7: Photocatalytic Activity of TAF Nps

3.8. Potential of bimetallic nanocomposite in Pharmacological Applications

3.8.1. Anti-inflammatory activity

The bimetallic nanoparticles have excellent properties than the monometallic nanoparticles. Due to their enlarged surface area and adaptability in medicinal fields[64]. The

ethanolic leaves extract of the *Clitoria ternatea* was used as the capping agent which reduces the higher oxidation state to the stable lower oxidation state monometallic and bimetallic nanocomposites. The synthesized NPs were evaluated and compared using cell-based assays for the anti-inflammatory efficacy as shown in Table-3. The reports were expressed based on the IC50 (the concentration that caused 50% inhibition) which were tabulated in Table-3. In *in vitro* measurements observed in anti-inflammatory efficacy for the synthesized bimetallic nanocomposites at various concentrations (500, 250, 100, 50 and 10 µg/ mL) exhibits a good efficacy at 500 µg/mL. TAF nanocomposites were found to inhibit the denaturation of albumin. On heating, TAF NPs containing the reaction mixture had no cloudy appearance and precipitation while the egg albumin in the absence of TAF NPs on heating gives white precipitation. Thus, denaturisation of egg albumin and IC50 value has been measured and tabulated.

Table-3: Inhibition percentage of albumin denaturation (%)

S. No	**Tested sample concentration (µg/ml)**	**Inhibition percentage albumin denaturation (%) (in triplicates)**			**Mean Value (%)**
1.	Control	100	100	100	100
2.	500 µg/ml	46.94444	43.61111	41.11111	43.88889
3.	250 µg/ml	39.16667	37.77778	36.94444	37.96296
4.	100 µg/ml	35.83333	35	30.83333	33.88889
5.	50 µg/ml	30.00	29.72222	29.72222	29.81481
6.	10 µg/ml	29.16667	1.388889	19.44444	16.66667

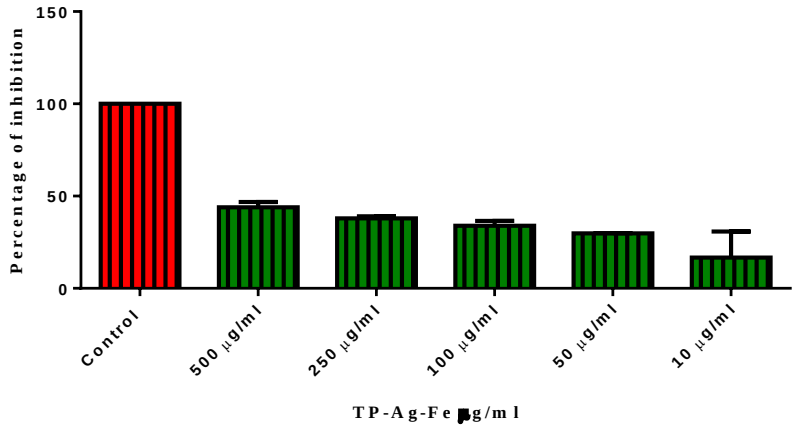

Figure-8: Bar Diagram representation of Inhibition percentage of TAF Nps

3.8.2. Inhibition of Enzymatic Activity of α-Amylase by TAF NPs

The inhibition of pancreatic α-amylase and intestinal α-glucosidase the two digestive enzymes is specifically useful for the treatment of non-insulin diabetes. It will slow down the release of glucose in the blood and regulates the diabetic condition [65-66].

In the alpha-amylase assay, the less intense red color declared synthesized BAF NPs as an alpha-amylase enzyme inhibitor. The activity is carried out in a various dosages of the the synthesized bimetallic nanocomposite. The maximum inhibition revealed by TAF NPs was 11.25%, and the standard drug acarbose exhibited 39% inhibition. The IC50 values calculated from the regression equation for TAF NPs (IC50- 90.82) respectively. The results illustrate the dominant capability of biosynthesized TAF NPs as an antidiabetic agent over reference drugs with significant values shown in Table-4.

S. No.	**Tested sample concentration (µg/ml)**	**Inhibition** (%)
1.	Acarbose	39.27
2.	500 µg/ml	11.25
3.	250 µg/ml	8.03
4.	100 µg/ml	6.96

5.	50 µg/ml	4.48
6.	10 µg/ml	1.25

Table-4: Inhibition of Enzymatic Activity of α-Amylase by TAF NPs

3.8.3. Antibacterial activity

The antibacterial potential of TAF NPs against *Aeromonas hydrophila, Staphylococcus aureus, Proteus vulgaris and Streptococcus pyogenes* were investigated. TAF NPs was found to be the toxic species to inhibit the growth of *A. hydrophila, S. aureus, P. vulgaris and S. pyogenes*. The growth of the bacterial specimens was completely inhibited by the TAF Nps for various concentrations. The maximum antibacterial potential was found at 500 µg/ml of the synthesized bimetallic nanocomposites for all the bacterial specimens. The maximum inhibition zone 20.5 mm was observed for TAF NPs against *Aeromonas hydrophila* depicted in Fig.10. In addition, the silver ions released from TAF NPs plays a vital role of the antibacterial potential due to the interaction of silver ion and iron ion [67].

Table-5: SD± Means of zone of inhibition obtained by sample TAF Nps against bacterial species

S. No	Name of the test organism	Zone of inhibition (mm) SD ± Mean				
		500 µg/ml	**250 µg/ml**	**100 µg/ml**	**50 µg/ml**	**PC**
1.	*Aeromonas hydrophila*	20.5±0.7	17.5±0.7	5.5±0.7	4.25±0.35	24.5± 0.7
2.	*Proteus vulgaris*	12.5±0.7	9.25±0.435	0	0	7.5±0.7
3	*Staphylococcus aureus*	12.5±0.7	10.5±0.7	4.25± 0.35	0	16.5± 0.7
4.	*Streptococcus pyogenes*	12.25± 0.35	11.25±0.35	0	0	15.5± 0.7

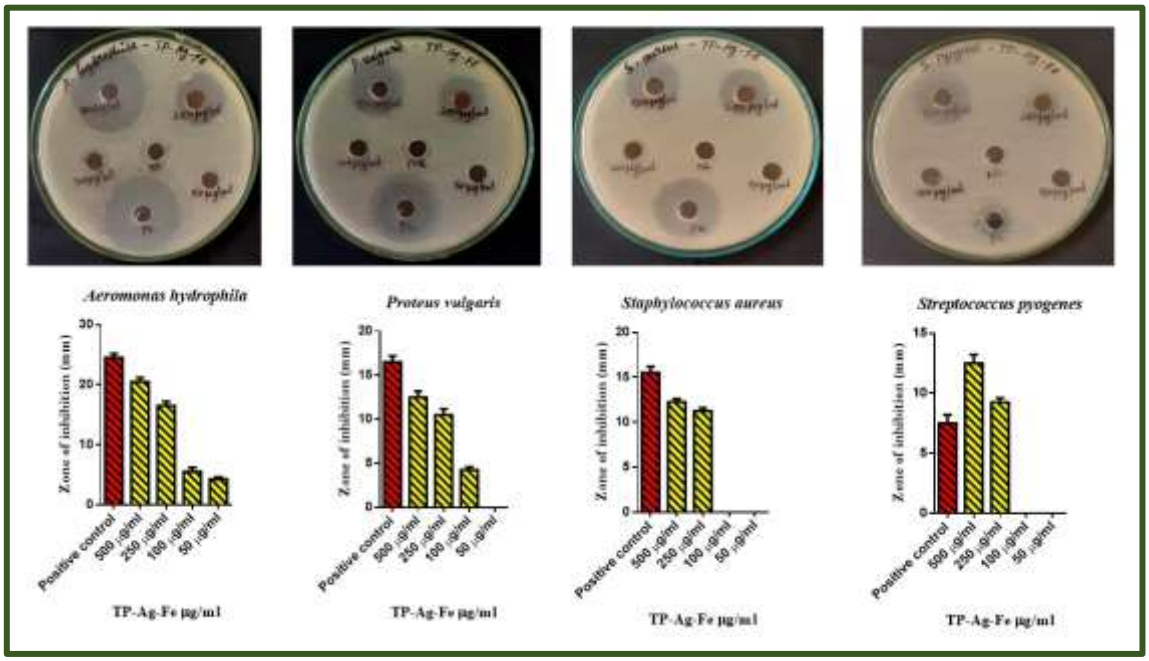

Figure-11: Zone of inhibition obtained by sample TAF Nps against bacterial species

3.8.4. Antifungal activity

The antifungal efficacy of TAF NPs against *Candida albicans, Aspergillus aculeatus, Aspergillus niger* and *Cryptococccus neoformans* were investigated. TAF NPs was found to be the toxic to the growth of *fungal species*. The *C. albicans*, *A. aculeatus*, *A. niger* and *C. neoformans* growth was inhibited by the TAF NPs. The synthesized nanoparticles were taken in different concentrations and antifungal efficacy is investigated by well diffusion method. The maximum inhibition zone 17.5 mm was observed for TAF NPs against *Aspergillus aculeatus* depicted in Fig.12. On comparing inhibition zone measure against the fungal species the synthesized bimetallic nanoparticles is a good antifungal agent.

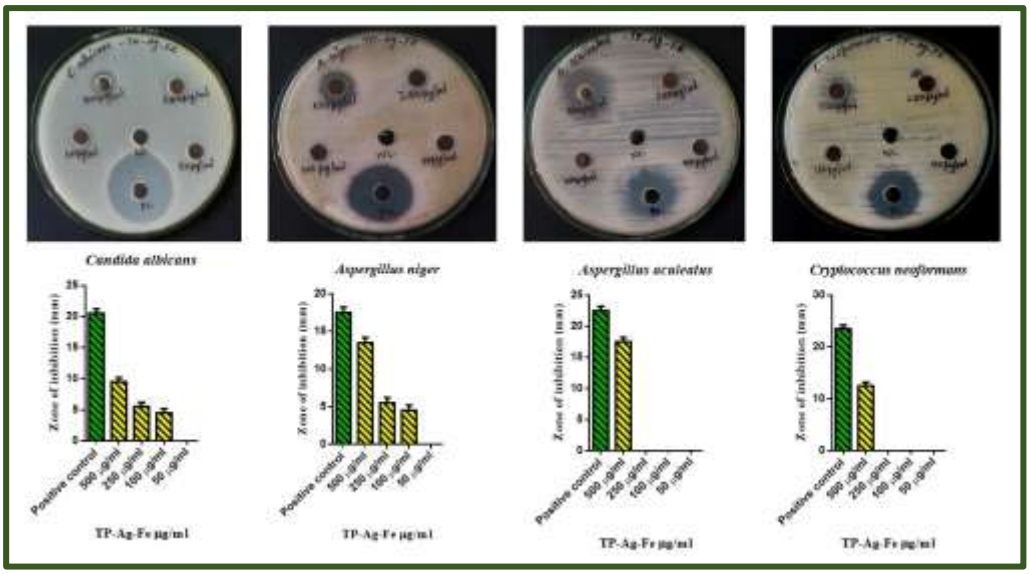

Figure-12: Zone of inhibition obtained by sample BAF Nps against fungal species

Table-6: SD± Means of zone of inhibition obtained by sample TAF Nps against *fungal species*

S.NO	Name of the test organism	Zone of inhibition (mm) SD ± Mean				
		500 µg/ml	**250 µg/ml**	**100 µg/ml**	**50 µg/ml**	**PC**
1.	*Candida albicans*	9.5±0.7	5.5±0.7	4.5±0.7	0	20.5± 0.7
2.	*Aspergillus niger*	13.5±0.7	5.5±0.7	4.5±0.7	0	17.5± 0.7
3.	*Aspergillus aculeatus*	17.5±0.7	0	0	0	22.5± 0.7
4.	*Cryptococcus neoformans*	12.5±0.7	0	0	0	23.5± 0.7

3.8.5. Anti-Biofilm Assay

The minimum inhibitory concentration values are used to determine susceptibilities of bacteria *Enterococcus faecalis* (MTCC. No. 439) to the drug TAF NPs. The anti-biofilm investigation involves in determining the potential of the synthesized bimetallic nanocomposite at different concentrations based on IC50 value. The maximum inhibitory

potential was at the higher concentration of TAF NPs 500 µg/ml- 68.60. The investigation of the formation of the biofilm under deprived conditions indicated the obvious signs for the surface degradation of dentine. This degradation is the sign of interactions between the TAF NPs and the bacterial cells. This report clearly shows the capability of *E. faecalis* to resist nutrient starvation for a long period[68-69].

Table-7: Percentage of *Biofilm inhibition*

S. No	Tested sample concentration (µg/ml)	Mean value (%)
1.	Control	89.79644
2.	500 µg/ml	68.60051
3.	250 µg/ml	64.35115
4.	125 µg/ml	35.87786
5.	62.5 µg/ml	21.14504
6.	31.25 µg/ml	10.40712

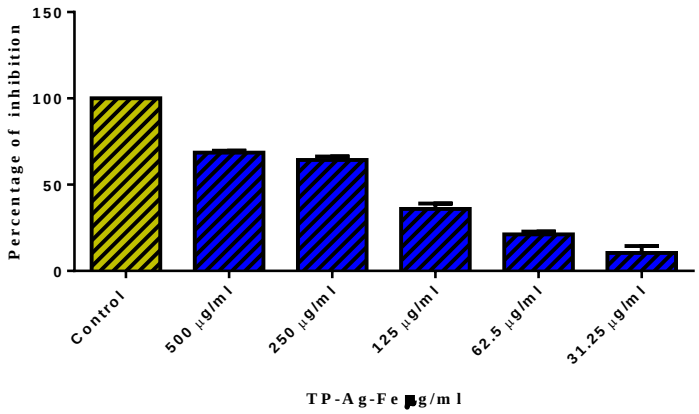

Figure-13: Zone of inhibition obtained by sample TAF Nps against Bioflim formation

4. Conclusion

Thus from the reports of the results obtained concludes that the monometallic and bimetallic nanocomposites such as Ag Nps (TA), Fe Nps(TF) and Ag-Fe (TAF) Nps were facile bio-fabricated from the ethanolic leaves extract of *Clitoria ternatea* as bio-reductant

and characterized by various spectral analyses. The respective peaks and bands obtained in UV-visible and FTIR spectra confirms the formation of core shell Ag-Fe NPs. The SEM images clearly depicts and confirms the formation of spherical and flakes like particles of the Ag-Fe NPs. The fabricated TAF NPs were taken for various applications for its good and active pharmacological efficacy as anti-diabetics, anti-inflammatory, anti-bacterial, antifungal and anti-biofilm formation. Thus the synthesized TAF NPs holds good as a concentration and time dependent photo-catalyst for the removal of methy red dye. Thus it is concluded that the bio fabricated monometallic and bimetallic nanoparticles using *Clitoria ternatea* as bio-reductant by co-precipitation method has many industrial and pharmacological applications.

Consent to Publish

Not applicable

Authors Contribution

The author PV analysis the all data in this manuscript. The PV and SS were contributed equally to preparing the manuscript.

Funding

Not applicable

Declaration

The authors declare that they have no conflict of interest

Competing Interests

The authors have no relevant financial or non-financial interests to disclose

Availability of data and materials

Not applicable

References

1. Karn, B.P., Bergeson, L.L., *Nat. Res. Environ.*,2009.
2. Sukanchan Palit and Chaudhery Mustansar Hussain., Recent Advances in Green Nanotechnology and the Vision for the Future., Department of Chemical Engineering-*University of petroleum*.,2018.

3. Mittal, A., Naushad, M., Sharma, G., Alothman, Z.A., Wabaidur, S.M., Alam, M., *Desalination and Water Treatment*., 2016.
4. Pankhurst, Q.A., Connolly, J., Jones, S.K., Dobson, J.J, *J. Phys. D. Appl. Phys*., 2003.
5. A. Z. Wang, F. Gu, L. Zhang, J. M. Chan, A. Radovic-Moreno, M. R. Shaikh, O. C. Farokhzad, *Expert Opin. Biol. Ther.* 8 (2008) 1063–1070.
6. K. N. Thakkar, S. S. Mhatre, R. Y. Parikh, *Nanomedicine Nanotechnology, Biol. Med.* 6 (2010) 257–262.
7. D. S. Goodsell, *Bionanotechnology: Lessons from Nature*, Wiley- Liss, Hoboken, NJ, USA, 2004.
8. S. Pal, Y. K. Tak, and J.M. Song, "Does the antibacterial activity of silver nanoparticles depend on the shape of the nanoparticle? A study of the gram-negative bacterium *Escherichia coli*," *AppliedandEnvironmentalMicrobiology*, vol. 73,no. 6, pp. 1712–1720, 2007.
9. R. Malhotra, "Mass spectroscopy in life sciences," *Current Science*, vol. 98, pp. 140–145, 2010.
10. N. Prabhu, D. T. Raj, K. Yamuna Gowri, S. Ayisha Siddiqua, and D. Joseph Puspha Innocent, "Synthesis of silver phyto nanoparticles and their antibacterial efficacy," *Digest Journal of Nanomaterials and Biostructures*, vol. 5, no. 1, pp. 185–189, 2010.
11. S. Balaji, *Nanobiotechnology*, MJP Publishers, Chennai, India, 2010. Journal of Nanoscience 7
12. B. Nair and T. Pradeep, "Coalescence of nanoclusters and the formation of sub-micron crystallites assisted by *Lactobacillus* strains," *Crystal Growth and Design*, vol. 2, no. 4, pp. 293–298, 2002.
13. J. B. Fathima, A. Pugazhendhi, R. Venis, *Microb. Pathog.* 110 (2017) 245–251.
14. D. Li, Z. Liu, Y. Yuan, Y. Liu, F. Niu, *Process Biochem.* 50 (2015) 357–366.
15. V. S. Ramkumar, A. Pugazhendhi, K. Gopalakrishnan, P. Sivagurunathan, G. D. Saratale, T. N. B. Dung, E. Kannapiran, *Biotechnol. Reports* 14 (2017) 1– 7.
16. Q. Zhang, J. M. Shreeve, *Chem. Rev.* 114 (2014) 10527–10574.
17. A. Z. Wang, F. Gu, L. Zhang, J. M. Chan, A. Radovic-Moreno, M. R. Shaikh, O.C. Farokhzad, *Expert Opin. Biol. Ther.* 8 (2008) 1063–1070.https://doi.org/10.1517/14712598.8.8.1063.

18. Z. U. H. Khan, A. Khan, Y. Chen, N. S. Shah, N. Muhammad, A. U. Khan, K. Tahir, F. U. Khan, B. Murtaza, S. U. Hassan, *J. Photochem. Photobiol. B Biol.* 173 (2017) 150–164.
19. A. A. Ostroushko, M. O. Tonkushina, *Russ. J. Phys. Chem. A* 89 (2015) 443–446.
20. E. C. Nnadozie, P. A. Ajibade, *Mater. Lett.* 263 (2020) 127145.
21. K. U. Sivakami, S. Vaideeswaran, A. R. Venis, J. K. A. J. Helina, M. Balaganesh, *Mater. Lett. X* 13 (2022) 100134.
22. M. M. S. Abdullah, A. M. Atta, H. A. Allohedan, H. Z. Alkhathlan, M. Khan, A. O. Ezzat, *Nanomaterials* 8 (2018) 855.
23. S. Venkateswarlu, B. N. Kumar, C. H. Prasad, P. Venkateswarlu, N. V. V Jyothi, *Phys. B Condens. Matter* 449 (2014) 67–71.
24. H. Agarwal, S. V. Kumar, S. Rajeshkumar, *Resour. Technol.* 3 (2017) 406–413.
25. M. Mokhtary, M. Torabi, *J. Saudi Chem. Soc.* 21 (2017) S299–S304.
26. P. Mukherjee, A. Ahmad, D. Mandal et al., "Fungus-mediated synthesis of silver nanoparticles and their immobilization in themycelialmatrix: a novel biological approach to nanoparticle synthesis," *Nano Letters*, vol. 1, no. 10, pp. 515–519, 2001.
27. N. Dur´an, P. D. Marcato, O. L. Alves, G. I. H. De Souza, and E. Esposito, "Mechanistic aspects of biosynthesis of silver nanoparticles by several *Fusarium oxysporum* strains," *Journal of Nanobiotechnology*, vol. 3, article no. 8, 2005.
28. S. P. Chandran, M. Chaudhary, R. Pasricha, A. Ahmad, and M. Sastry, "Synthesis of gold nanotriangles and silver nanoparticles using *Aloevera* plant extract," *Biotechnology Progress*, vol. 22,no. 2, pp. 577–583, 2006.
29. S. Li, Y. Shen, A. Xie et al., "Green synthesis of silver nanoparticles using *Capsicum annuum* L. extract," *Green Chemistry*, vol.9, no. 8, pp. 852–858, 2007.
30. J. Huang, Q. Li, D. Sun et al., "Biosynthesis of silver and gold nanoparticles by novel sundried *Cinnamomum camphora* leaf," *Nanotechnology*, vol. 18, no. 10, Article ID 105104, 2007.
31. S. Garima, B. Riju, K. Kunal, R. S. Ashish, and P. S. Rajendra, "Biosynthesis of silver nanoparticles using *Ocimum sanctum* (Tulsi) leaf extract and screening its antimicrobial activity," *Journal of Nanoparticle Research*, vol. 13, no. 7, pp. 2981–2988, 2011.
32. A. Singh, D. Jain,M. K. Upadhyay, N. Khandelwal, and H. N. Verma, "Green synthesis of silver nanoparticles using *Argemone Mexicana* leaf extract and evaluation

of their antimicrobial activities," *Digest Journal of Nanomaterials and Biostructures*, vol. 5, no. 2, pp. 483–489, 2010.

33. D. V. Parikh, T. Fink, K. Rajasekharan et al., "Antimicrobial silver/sodium carboxymethyl cotton dressings for burn wounds," *Textile Research Journal*, vol. 75, no. 2, pp. 134–138, 2005.
34. V. Alt, T. Bechert, P. Steinr¨ucke et al., "An in vitro assessment of the antibacterial properties and cytotoxicity of nanoparticulate silver bone cement," *Biomaterials*, vol. 25, no. 18, pp. 4383–4391, 2004.
35. G. Gosheger, J.Hardes, H. Ahrens et al., "Silver-coated megaendoprostheses in a rabbitmodel—an analysis of the infection rate and toxicological side effects," *Biomaterials*, vol. 25, no. 24, pp. 5547–5556, 2004.
36. A. M Awwad, B. Albiss, A. L Ahmad, *Adv. Mater. Lett.* 5 (2014) 520–524.
37. S. K. Chaudhuri, L. Malodia, *Def. Life Sci J* 2 (2017) 65–73.
38. JK. Alphonsa Juliet Helina, G. Dayana Jeya Leela, V. AlexRamani, T. Francis Xavier and A. Auxilia, World Journal of Pharmacy and Pharmaceutical Sciences," Phytochemical screening and antimicrobial studies on the medicinal plant *Flueggea leucopyrus (Willd.)*", Volume 4, Issue 09, 717-726, 2015.
39. M. Herlekar, S. Barve, R. Kumar, *J. Nanoparticles* 2014 (2014)1-9.
40. F. Luo, D. Yang, Z. Chen, M. Megharaj, R. Naidu, *J. Hazard. Mater.* 303 (2016) 145–153.
41. D. Philip, *Spectrochim. Acta Part A Mol. Biomol. Spectrosc.* 73 (2009) 650–653.
42. I. Hussain, N. B. Singh, A. Singh, H. Singh, S. C. Singh, *Biotechnol. Lett.* 38 (2016) 545–560.https://doi.org/10.1007/s10529-015-2026-7.
43. K. Manojkumar, A. Sivaramakrishna, K. Vijayakrishna, *J. Nanoparticle Res.* 18 (2016) 103.https://doi.org/10.1007/s11051-016-3409-y.
44. M. Salavati-Niasari, J. Javidi, F. Davar, *Ultrason. Sonochem.* 17 (2010) 870–877.
45. S. Gupta, M. Lakshman, *J. Med. Chem. Sci.* 2 (2019) 51–54.J. K. A. J. Helina, I. A. Kumar, N. Viswanathan, *Mater. Today Proc.* (2021).
46. J. K. A. J. Helina, A. P. P. Regis, *Asian J. Pharm. Pharmacol.* 5 (2019) 111–119.
47. G. Maheshwaran, M. M. Selvi, R. S. Muneeswari, A. N. Bharathi, M. K. Kumar, S. Sudhahar, *Adv. Powder Technol.* 32 (2021) 1963–1971.
48. S. Gonca, S. Özdemir, A. Tekgül, C. G. Unlu, K. Ocakoglu, N. Dizge, *Adv. Powder Technol.* 33 (2022) 103346.

49. V. Vinotha, A. Iswarya, R. Thaya, M. Govindarajan, N. S. Alharbi, S. Kadaikunnan, J. M. Khaled, M. N. Al-Anbr, B. Vaseeharan, *J. Photochem. Photobiol. B Biol.* 197 (2019) 111541.
50. B. N. Rashmi, S. F. Harlapur, B. Avinash, C. R. Ravikumar, H. P. Nagaswarupa, M. R. A. Kumar, K. Gurushantha, M. S. Santosh, *Inorg. Chem. Commun.* 111 (2020) 107580.
51. Nagadeep J, Kamaraj P, Arthanareeswari M. Gradient RP-HPLC method for the determination of potential impurities in dabigatran etexilate in bulk drug and capsule formulations. Arabian Journal of Chemistry. 2019 Dec 1;12(8):3431-43.
52. Jaishetty N, Palanisamy K, Maruthapillai A, Jaishetty R. Trace Level Quantification of the (−) 2-(2-amino-5-chlorophenyl)-4-cyclopropyl-1, 1, 1-trifluoro-3-butyn-2-ol Genotoxic Impurity in Efavirenz Drug Substance and Drug Product Using LC–MS/MS. Scientia pharmaceutica. 2016;84(3):456-66.
53. Jaishetty N, Palanisamy K, Maruthapillai A. Enantiometric Separation Of Sitagliptin In A Fixed Dose Combination Formula Of Sitagliptin And Metformin By A Chiral Liquid Chromatographic Method. Int J Pharm Pharm Sci. 2019;8:30-4.
54. Kavitapu D, Jaishetty N, Maruthapillai A, Murty JN. Identification of Two Novel Hydroperoxide Impurities in Fluocinolone Acetonide Topical Solution by Liquid Chromatography Mass Spectrometry. Journal of Chromatographic Science. 2023 Jan 22:bmad003.
55. Alwera, Vijay, Nagadeep Jaishetty, Vladimir Sergeevich Talismanov, Munfis Samir Patel, Suman Sehlangia, and Shiv Alwera. "Pre-column Derivatization Elution Order, Molecular Configuration and Green Chromatographic Separation of Diastereomeric Derivatives of β-Amino Alcohols." (2022).
56. Nagadeep J, Kamaraj P, Arthanareeswari M, Vivekanand P. Identification of Tartaric Acid Adduct Impurities in Dipyridamole Capsule Formulation Related Substances Method. Asian Journal of Chemistry. 2021;33(2):307-13.
57. A. Lassoued, B. Dkhil, A. Gadri, S. Ammar, Results. Phys. **7**, 3007 (2017)
58. G. Prasanna, R. Anuradha, Asian. J. Pharm Clin. Res. **6**, 10 (2016)
59. M. Gotic, G. Koscec, S. Music, J. Mol. Struct. **924**, 347 (2009).
60. Patil, S.; Chandrasekaran, R. Biogenic nanoparticles: J. Genet. Eng. Biotechnol. 2020, 18, 67.
61. M. Dubay, S. Bhadauria, B. S. Kushwah, Dig J Nanomater Biostruct 2009, 4, 537-43.

62. Anna Podsędek, Iwona Majewska, Małgorzata Redzynia, Dorota Sosnowska, Maria Koziołkiewicz, J. Agric. Food Chem. 2014, 62, 4610−4617.
63. M. E. Rupp, T. Fitzgerald, N. Marion et al., "Effect of silvercoated urinary catheters: efficacy, cost-effectiveness, and antimicrobial resistance," *American Journal of Infection Control*, vol. 32, no. 8, pp. 445–450, 2004.
64. S. Ohashi, S. Saku, and K. Yamamoto, "Antibacterial activity of silver inorganic agent YDA filler," *Journal of Oral Rehabilitation*, vol. 31, no. 4, pp. 364–367, 2004.
65. M. Bosetti, A. Mass`e, E. Tobin, and M. Cannas, "Silver coated materials for external fixation devices: in vitro biocompatibility and genotoxicity," *Biomaterials*, vol. 23,no. 3, pp. 887–892, 2002.
66. H. J. Lee and S. H. Jeong, "Bacteriostasis and skin innoxiousness of nanosize silver colloids on textile fabrics," *Textile Research Journal*, vol. 75, no. 7, pp. 551–556, 2005.
67. Alphonsa Juliet Helina JK, I. Aswin Kumar and N. Viswanathan, "Fabrication and analysing *Drypetes sepairia* encapsulated chitosan hybrid beads as anticorrosion agent" Materials Today: Proceedings 47 (2021) 1929–1936.
68. N. Sap-Lam, C. Homklinchan, R. Larpudomlert, W. Warisnoicharoen, A. Sereemaspun, and S. T. Dubas, "UV irradiation induced silver nanoparticles as mosquito larvicides," *Journal of Applied Sciences*, vol. 10, no. 23, pp. 3132–3136, 2010.
69. C.Marambio-Jones andE.M. V. Hoek, "Areviewof the antibacterial effects of silver nanomaterials and potential implications for human health and the environment," *Journal of Nanoparticle Research*, vol. 12, no. 5, pp. 1531–1551, 2010.